



## Introducing an Enhanced Friction Model for Developing Inertia Welding Simulation: A Computational Solid Mechanics Approach

B. Meyghani<sup>\*a</sup>, M. Awang<sup>b</sup>, S. S. Emamian<sup>c</sup>

<sup>a</sup> Institute of Materials Joining, Shandong University, Jingshi Road, Jinan, China

<sup>b</sup> Department of Mechanical Engineering, Faculty of Engineering, Universiti Teknologi PETRONAS (UTP), Bandar Seri Iskandar, Perak Darul Ridzuan, Malaysia

<sup>c</sup> Center of Advance Manufacturing and Material Processing (AMMP), Department of Mechanical Engineering, Faculty of Engineering, University of Malaya, Malaysia

### PAPER INFO

#### Paper history:

Received 13 December 2020

Received in revised form 01 January 2021

Accepted 15 January 2021

#### Keywords:

Solid-state Welding

Friction Model

Coulomb Friction Model

Computational Solid Mechanics

### ABSTRACT

Numerical simulation of inertia welding attracts enormous research interest during the past decades. Extremely large plastic deformation and complicated frictional behavior make this simulation challenging. In this paper, Norton friction model is modified to be employed in a computational solid mechanics model of inertia welding. A continuous remeshing technique is used to avoid the mesh distortion problem. The results show that after 1.5 (s) the temperature reaches the maximum value of 1200 °C. After that, a decreasing pattern is found for the welding temperature. Moreover, the maximum deformation of 6 mm is obtained. The stress increased to the maximum values of 975 MPa. Consequently, successful prediction of the temperature distribution, thermal history, equivalent plastic deformation, axial shortening and stress distribution is made. The comparisons between the results of this study and the literature showed that implementing the proposed methodology leads to achieving high accuracy results.

doi: 10.5829/ije.2021.34.03c.19

## 1. INTRODUCTION

Inertia welding or inertia friction welding is a solid-state joining process that is considered as a suitable method for joining different materials together. In this welding, intimate contact of a plasticized at the welding interfaces produces by the frictional heat and the pressure. In order to achieve an accurate finite element modeling of the process, the implementation of the contact interface should be considered as a significant issue. Thus, different available models were presented by researchers [1, 2] for modeling the friction-based joining processes.

Different friction models are proposed by researchers for thermomechanical analysis of the solid-state joining processes such as inertia and friction stir welding (FSW) processes [3-5]. In these models, both computational solid mechanics (CSM) and computational fluid

dynamics (CFD) methods are used in different models. Here, it should be noted that CSM models that are based on finite element methods are mostly used for solving solid mechanics problems, while CFD models are based on finite volume methods and can be appropriate for solving fluid dynamics problems.

In the majority of the proposed CSM based finite element packages, Coulomb friction law is used. In the above-mentioned models, constant or limited ranges for the friction coefficient are employed because the Coulomb friction model is based on the sliding condition [6]. To illustrate the problem, due to the usage of the constant values for the friction coefficient [7, 8], the Coulomb friction model is limited to the sliding frictional condition where the temperature values are low [9]. Based on CSM, Shun et al. [10] employed the Coulomb friction law in DEFORM-3D finite element package for

\*Corresponding Author Institutional Email:  
[Bahman.meyghani@sdu.edu.cn](mailto:Bahman.meyghani@sdu.edu.cn) (B. Meyghani)

modeling the inertia welding process. Nimesh et al. used the Coulomb friction model for modeling the dissimilar inertia welding [11] in the Abaqus software environment; however, the model results were limited to the temperature prediction. Constant values of the friction are used in the Coulomb model to simulate FSW process to achieve an accurate prediction of the temperature [12]. From the above-mentioned descriptions, the Coulomb model cannot be accurate to simulate the inertia welding or FSW processes where a partial sliding/sticking condition is available [13]. Consequently, there is a need to use a complicated friction law for simulating the sticking behavior at the tool-workpiece interface.

Although in some limited cases there is an ability (like user-defined subroutines) to modify the package in order to use a more complicated friction model, these modifications are challenging because of the mesh distortion and thereby increasing the computational cost. To explain more, there are different techniques for mesh modeling, Lagrangian, Eulerian and arbitrary Lagrangian-Eulerian (ALE). ALE has been successful in solving the mesh distribution problem which is one of the key and significant difficulties during modeling large plastic deformation processes. However, the computational costs of the ALE method for employing a complicated friction model by user-defined subroutines are high. Norton friction model is proposed by some researchers [13, 14]. In this model, the shear stress is defined to be as a function of relative velocity between the tool velocity and the material velocity. It was claimed that in comparison to the Coulomb friction model, this model has higher accuracy. Another advantage of this model over Coulomb law is the avoidance of a constant value for the friction coefficient. Moreover, in this model the ratio between the shear stress and the pressure is defined as a complicated function of the interface relative velocity (the difference between the velocity of the tool and the material flow velocity). In some model CFD models, Norton friction law is used to achieve a partial sliding sticking condition. They [4, 14] used Norton friction law in the case of sticking condition. These researchers also claim that this formulation can be appropriate for modeling the FSW. As discussed, the majority of the above-mentioned researchers used CFD models, because it can easily handle the distribution of the mesh and its computational costs are low. Here, it should be noted that, the accuracy of the CSM for modeling the inertia welding leads to achieving higher accuracy and efficiency. To illustrate, CSM deals with both mathematical modeling and numerical simulation of solid related phenomena. Thus, these methods can be appropriate for modeling inertia welding. From the above-mentioned descriptions, it can be claimed that accurate implementation of the friction law in the CSM models is mandatory.

Up to now, quite a few models have been developed

to analyze the heat generation, temperature field, plastic deformation and stress in inertia welding quantitatively. Moreover, all proposed models used the Eulerian formulation in CFD models. It should be noted that there are limitations in predicting the strain rate and residual stress for CFD-based models. In the case of using an Eulerian based CSM models, implementing a complicated friction mode, overcoming the mesh distortion and reducing the computational costs are significant challenges.

In this paper, the Norton-Hoff viscoplastic law is modified in order to investigate the relative velocity between the workpieces. Then, a novel method is used to implement this modified friction law to a three-dimensional finite element model (FEM) model. A proper continuous remeshing method is also employed to avoid the distortion of mesh and decreasing the computational costs. Finally, the model is validated by comparing the results of the FE model with experimental tests and the data in the literature.

## 2. Materials and Methods

### 2. 1. Interaction Definitions

Five different conditions and one actuator-sensor for the interaction section are defined at the welding interfaces. The constant workpiece is considered to be the master surface and the rotating one is considered to be the slave surface. Two different user-defined subroutines are applied to the model. The first one (Fric) is applied to implement the Norton friction model at the interfaces. A prescribed pressure of 360 MPa is also applied to complete the treatment of friction force. Thus, the generation of the heat is based on the traction and the sliding velocity. The second subroutine UEL is applied as an actuator-sensor. As mentioned, the modified Norton friction model is used in this model that is based on the friction law proposed by Moal and Massoni [15]. Equation 1 shows the general form of the model.

$$\tau = -P \times g(\Delta v_g) \times \frac{\Delta v_g}{|\Delta v_g|} \quad (1)$$

where  $\tau$  is the shear stress,  $P$  is the prescribed pressure and  $g(\Delta v_g)$  is the defined function for the ratio between the tool velocity and the material velocity.

It should be noted that Equation 1 is calculated based on the experiments done by Moal and Massoni [15]. In this equation the ratio between the shear stress and the pressure ( $\tau/P$ ) is equal to the relative velocity function. Different conditions are defined for the relative velocity function ( $g(\Delta v_g)$ ) [16, 17]. These conditions are based on the difference between the velocity of the tool and the material velocity at each point and each increment. A sticking condition is proposed near the tool-workpiece interface, where the relative velocity is not high [18]. Far

from the welding tool, a sliding condition is proposed. In this sliding condition, a constant value for the ratio between the shear and the pressure is considered, while a complicated polynominal function is considered for the sticking condition.

**2. 1. Finite Element Model Descriptions** A fully coupled temperature displacement analysis is selected as the analysis type [19, 20]. Two deformable parts are defined for the workpieces. The element type of CGAX4HT and CGAX3HT are selected for the simulation. The remeshing technique is also employed to avoid mesh distortion [21, 22]. In order to approximate the high-temperature behavior for Astroloy, the Norton-Hoff constitutive law is proposed to explain the complicated temperature and strain rate viscoplastic behavior. It needs to be explained that a rate dependent perfectly plastic material model is also defined [23]. Figure 1 shows a brief explanation for the initial model of the welding in a 2-dimensional viewpoint. Moreover, the room temperature of 20 °C is defined as the initial temperature [24, 25]. The initial rotating velocity for the workpiece is defined to be 48.17 radians per second and the mass moment of inertia of 102,000 Mg mm<sup>2</sup> is applied to the model.

**3. RESULTS AND DISCUSSION**

As mentioned earlier, two different subroutines are used to simulate the welding. At each step of the welding, the mesh converts to the geometry, then a new meshing applies for the new geometry (deformed geometry). It should be noted that all of the calculated results (temperature, stress, strains, etc.) at each step will be mapped and considered as new boundary conditions for the next step.

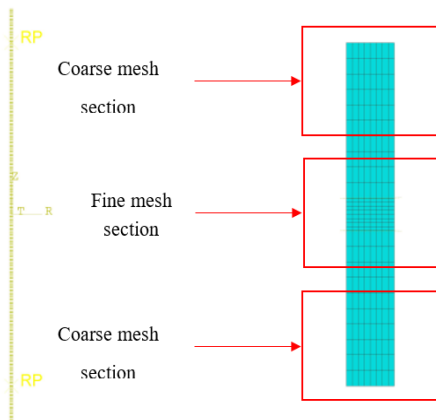


**Figure 1.** Schematic view and the initial mesh for the workpiece

**3. 1. Temperature Distribution** The distribution of the temperature in 2 and 3-dimensional viewpoints are shown in Figure 2. As can be seen in Figure 2 section a, the upset is formed successfully and accurately. The contour plot shows the temperature of 1103 °C at the interface between two pipes. The achieved values of the temperature are confirmed by the literature [26]. The temperature decreases along with the fully plastic deformed zone (the maximum temperature of 1011 °C). Far from the welding interface, the temperature has a decreasing rate pattern, because of the distance from the heat source. The main reason for this issue is the conduction, which transfers the heat along with the welding interface [27]. Moreover, due to the continuous remeshing, the mesh distortion problem is solved properly. From Figure 2, it can be seen that there is an extrude flash near the welding interface. This issue is also reported in the literature [27].

Figure 3 indicates the relationship between the time and the temperature at the welding interface. As can be seen, the temperature values sharply increase up to 1200 °C after 1.5 (s) of the welding. This indicates that the main source for the generating of the heat is the frictional force at the welding interface. Due to the implementation of an accurate frictional model in this study, the temperature pattern is in line with the literature [28]. This sharp increase in the values of temperature softens the

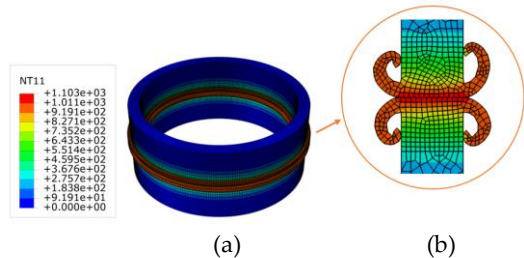


**Figure 2.** The temperature distribution a) three dimensional and the welding zone b) cross section of the welding

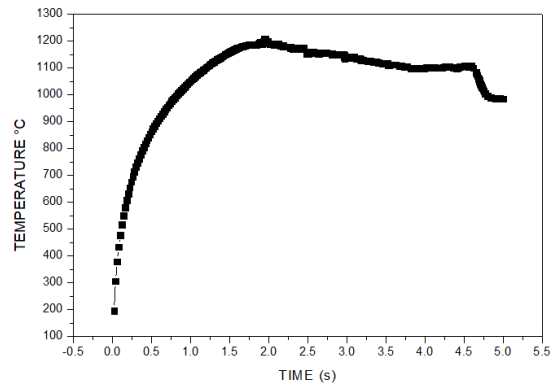


**Figure 3.** Temperature history at the welding interface

material, and make the deformation of the interface material easier. It can also be observed that a periodic fluctuation of temperature has happened during welding.

The contour plots of the temperature history are shown in Figure 4. As can be seen, after starting the welding (Figure 4-a), the temperature increases to the maximum value of 1178 °C. Applying a high pressure at the beginning of the welding can be the main reason for this sharp increasing rate for the temperature. Figure 4-b shows that with increasing the welding time, the temperature values decrease to 1150°C. It is obvious from Figure 4-c (at 1109 °C) and Figure 4-d (at 1150 °C) that the temperature is decreased as the welding continues. This is happening because of the increase in the amount of the transferred heat from radiation and convection. It should be noted that as the area of the fully plastic deformed zone increases, the heat transfer by radiation and convection increases as well, thus the welding interface temperature decreases. This phenomenon is also reported in the literature [29], which shows the accuracy of the results of this study.

**3. 2. Equivalent Plastic Strain** Figure 5 shows the relationship between the shortening of the welding interface and time. As can be seen, before achieving the peak temperature, the workpiece did not deform significantly. After 1.5 (s) the deformation begins and followed a sharp increasing pattern. To illustrate, the deformation sharply increased from 0 to 5 mm until the step time of 4.5 (s) (where the pressure is relieved from the pipes). This issue means that the length of the pipes decreases almost around 5 mm. From the welding time of 4.5 (s) to 5 (s) the deformation rate becomes constant, due to decreasing the pressure on the pipes. Comparisons with the data in literature show that the results of this section are in good agreement with the literature [30].

The equivalent plastic strain during the welding in 2 and 3 dimensions are shown in Figure 6-a. It is obvious

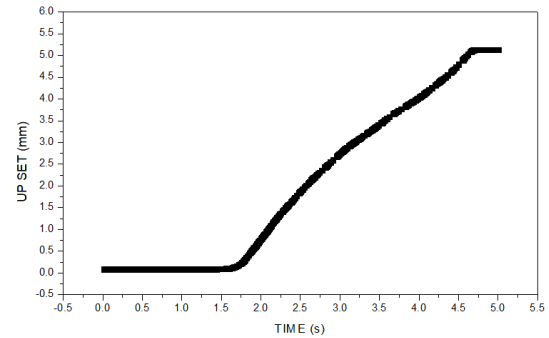


**Figure 5.** The relationship between the shortening and the time at the welding interface

that the maximum plastic strain is happening at the center of the welding, where two plates are joining together. Achieving the highest plastic deformation in this area is happening because the maximum temperature is located in this area. The plastic deformation decreases far from the welding interface (where the temperature drops gradually). This shows that there is a proportional relationship between plastic deformation and temperature. Figure 6 also indicates plastic deformation history. The results show that with increasing the welding time, the equivalent plastic deformation increases as well. As can be seen in Figure 6-e the maximum plastic deformation is happening in the peripheral regions. An almost asymmetric pattern for the upper and lower surfaces is achieved at the equilibrium stage. From the results of the fully plastic deformation zone, it is obvious

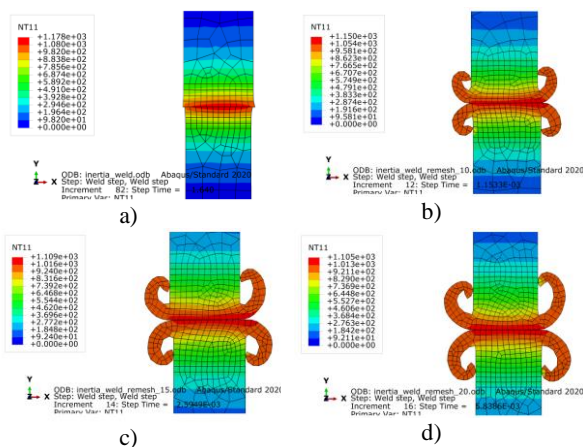


**Figure 4.** Contour plot of the temperature distribution history

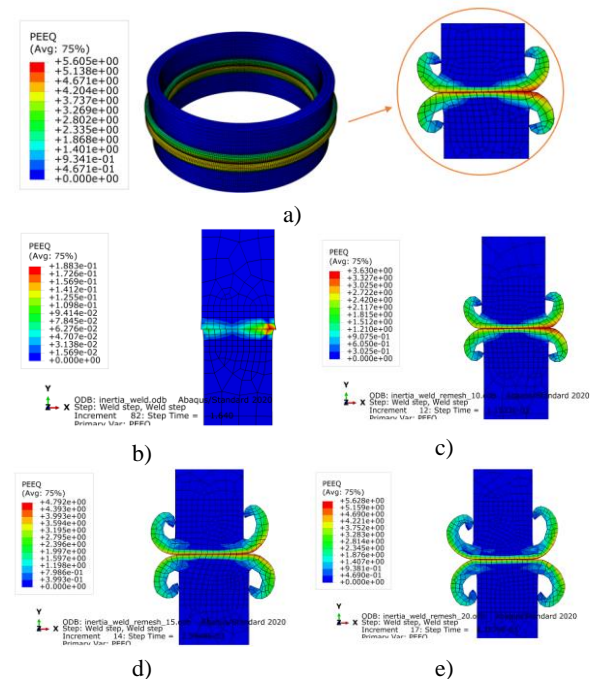


**Figure 6.** Equivalent plastic strain distribution

that the remeshing technique could accurately handle the mesh distortion problem.

**3.3. Stress Distribution** The stress distribution is one of the most significant issues during inertia welding, thus in the last part of the results and discussion section, this issue is addressed. Figure 7-a shows the distribution of the stress field in 2 and 3-dimensional viewpoints. The stress history also can be seen from Figure 7-b to Figure 7-e. The decreasing values of the stress at the welding are caused because of the decrease in the temperature. This matter indicates that, like the plastic deformation, there is a proportional relationship between the stress and the temperature. The stress distribution has an almost symmetrical pattern at the welding interface. As the distance from the welding interface increases, this symmetrical pattern changes to an almost asymmetrical shape. The maximum values of the stress are observed to be around 975 MPa (at the fully plastic deformed zone). It should be noted that the stress behavior is in good agreement with the achieved results in the literature [31].

#### 4. CONCLUSIONS

In this paper, a modified Norton friction model is proposed for finite element modeling of the inertia welding process. A continuous remeshing technique is also employed to avoid mesh distortions.

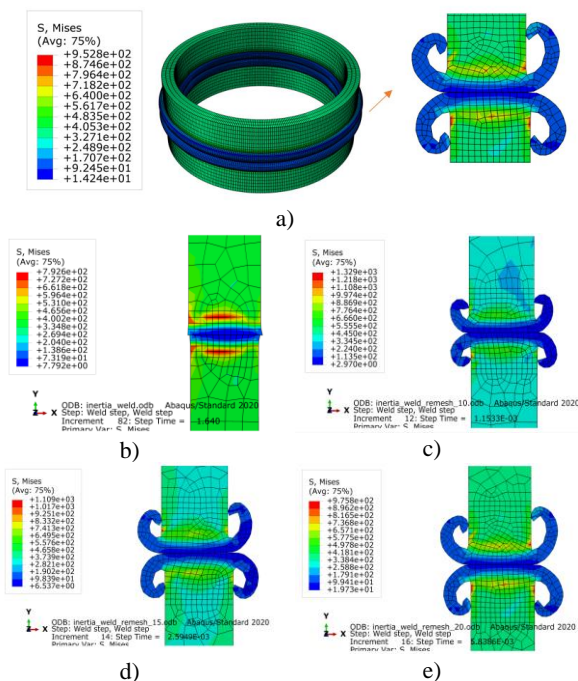


Figure 7. The distribution of the stress during welding

The summary of the findings can be concluded as below:

- The maximum temperature of 1200 °C is reached at the welding interface (at the welding time of 1.5 seconds).
- After that, the temperature decreased due to the increase of the radiation and convection heat transfer from the workpiece to the outside region.
- At the welding interface, the maximum deformation of 6 mm is observed.
- The maximum values of 975 MPa for the stress is achieved.
- Equivalent plastic deformation and stress are found to have an almost symmetrical pattern.
- A proportional relationship between the temperature and both the plastic deformation and stress is obtained.
- Comparisons showed a good agreement between the results of this study and the previous literature.

#### 5. REFERENCES

1. Buffa, G., Fratini, L., Impero, F., Masnata, A., Scherillo, F. and Squillace, A., "Surface and mechanical characterization of stationary shoulder friction stir welded lap joints: Experimental and numerical approach", *International Journal of Material Forming*, Vol., (2020), 1-12. <https://doi.org/10.1007/s12289-020-01574-9>
2. Sun, Z., Wu, C. and Kumar, S., "Determination of heat generation by correlating the interfacial friction stress with temperature in friction stir welding", *Journal of Manufacturing Processes*, Vol. 31, (2018), 801-811. <https://doi.org/10.1016/j.jmapro.2018.01.010>
3. Meyghani, B., Awang, M.B., Emamian, S.S., Mohd Nor, M.K.B. and Pedapati, S.R., "A comparison of different finite element methods in the thermal analysis of friction stir welding (fsw)", *Metals*, Vol. 7, No. 10, (2017), 450. <https://doi.org/10.3390/met7100450>
4. Meyghani, B. and Wu, C., "Progress in thermomechanical analysis of friction stir welding", *Chinese Journal of Mechanical Engineering*, Vol. 33, No. 1, (2020), 12. <https://doi.org/10.1186/s10033-020-0434-7>
5. Miles, M., Nelson, T., Gunter, C., Liu, F., Fourment, L. and Mathis, T., "Predicting recrystallized grain size in friction stir processed 304l stainless steel", *Journal of Materials Science & Technology*, Vol. 35, No. 4, (2019), 491-498. <https://doi.org/10.1016/j.jmst.2018.10.021>
6. Meyghani, B., Awang, M.B., Momeni, M. and Rynkovskaya, M., "Development of a finite element model for thermal analysis of friction stir welding (fsw)", in IOP Conference Series: Materials Science and Engineering, IOP Publishing. Vol. 495, (2019), 012101. Doi:10.1088/1757-899X/495/1/012101
7. Meyghani, B., Awang, M. and Emamian, S., "A mathematical formulation for calculating temperature dependent friction coefficient values: Application in friction stir welding (fsw)", in Defect and Diffusion Forum, Trans Tech Publ. Vol. 379, (2017), 73-82. <https://doi.org/10.4028/www.scientific.net/DDF.379.73>
8. Meyghani, B., Awang, M.B., Poshteh, R.G.M., Momeni, M., Kakooei, S. and Hamdi, Z., "The effect of friction coefficient in thermal analysis of friction stir welding (FSW)", in IOP Conference Series: Materials Science and Engineering, IOP

- Publishing. Vol. 495, (2019), 012102. Doi:10.1088/1757-899X/495/1/012102
9. Dialami, N., Cervera, M., Chiumenti, M. and de Saracibar, C.A., "Local-global strategy for the prediction of residual stresses in fsw processes", *The International Journal of Advanced Manufacturing Technology*, Vol. 88, No. 9, (2017), 3099-3111. <https://doi.org/10.1007/s00170-016-9016-3>
  10. Ji, S.-d., Liu, J.-g., Yue, Y.-m., Zan, L. and Li, F., "3d numerical analysis of material flow behavior and flash formation of 45# steel in continuous drive friction welding", *Transactions of Nonferrous Metals Society of China*, Vol. 22, (2012), s528-s533. [https://doi.org/10.1016/S1003-6326\(12\)61756-7](https://doi.org/10.1016/S1003-6326(12)61756-7)
  11. NIMESH, P., "Simulation of inertia friction welding of mild steel and aluminium 6061 using finite element method on abaqus", (2016).
  12. Meyghani, B., Awang, M. and Wu, C., "Thermal analysis of friction stir welding with a complex curved welding seam (technical note)", *International Journal of Engineering, Transactions A: Basics*, Vol. 32, No. 10, (2019), 1480-1484. <https://dx.doi.org/10.5829/ije.2019.32.10a.17>
  13. Dialami, N., Cervera, M., Chiumenti, M., Segatori, A. and Osikowicz, W., "Experimental validation of an fsw model with an enhanced friction law: Application to a threaded cylindrical pin tool", *Metals*, Vol. 7, No. 11, (2017), 491. <https://doi.org/10.3390/met7110491>
  14. Dialami, N., Cervera, M., Chiumenti, M. and de Saracibar, C.A., "A fast and accurate two-stage strategy to evaluate the effect of the pin tool profile on metal flow, torque and forces in friction stir welding", *International Journal of Mechanical Sciences*, Vol. 122, (2017), 215-227. <https://doi.org/10.1016/j.ijmecs.2016.12.016>
  15. Moal, A. and Massoni, E., "Finite element simulation of the inertia welding of two similar parts", *Engineering Computations*, (1995). <https://doi.org/10.1108/02644409510799730>
  16. MEYGHANI, B., "Thermomechanical analysis of friction stir welding (fsw) on curved plates by adapting calculated temperature dependent properties", Universiti Teknologi PETRONAS, (2018),
  17. Meyghani, B. and Awang, M., "A comparison between the flat and the curved friction stir welding (fsw) thermomechanical behaviour", *Archives of Computational Methods in Engineering*, (2019), 1-14. <https://doi.org/10.1007/s11831-019-09319-x>
  18. Meyghani, B., Awang, M. and Wu, C., "Finite element modeling of friction stir welding (fsw) on a complex curved plate", *Journal of Advanced Joining Processes*, Vol. 1, (2020), 100007. <https://doi.org/10.1016/j.jajp.2020.100007>
  19. Meyghani, B., Awang, M., Emamian, S. and Akinlabi, E., "A comparison between temperature dependent and constant young's modulus values in investigating the effect of the process parameters on thermal behaviour during friction stir welding: Vergleich zwischen den temperaturabhängigen und konstanten elastizitätsmodulwerten in der untersuchung der prozessparameter auf die wärmewirkung beim rührreibschweißen", *Materialwissenschaft und Werkstofftechnik*, Vol. 49, No. 4, (2018), 427-434. <https://doi.org/10.1002/mawe.201700255>
  20. Meyghani, B., Awang, M., Emamian, S. and Khalid, N.M., "Developing a finite element model for thermal analysis of friction stir welding by calculating temperature dependent friction coefficient", in 2nd International Conference on Mechanical, Manufacturing and Process Plant Engineering, Springer. (2017), 107-126. [https://doi.org/10.1007/978-981-13-8297-0\\_64](https://doi.org/10.1007/978-981-13-8297-0_64)
  21. Meyghani, B., Awang, M., Emamian, S. and Nor, M.K.B.M., Thermal modelling of friction stir welding (FSW) using calculated young's modulus values, in The advances in joining technology. 2018, Springer.1-13. [https://doi.org/10.1007/978-981-10-9041-7\\_1](https://doi.org/10.1007/978-981-10-9041-7_1)
  22. Meyghani, B., Awang, M. and Emamian, S., "A comparative study of finite element analysis for friction stir welding application", *ARP Journal of Engineering and Applied Sciences*, Vol. 11, No. 22, (2016), 12984-12989.
  23. Meyghani, B., Awang, M. and Wu, C., "Thermal analysis of friction stir processing (FSP) using arbitrary lagrangian-eulerian (ALE) and smoothed particle hydrodynamics (SPH) meshing techniques", *Materialwissenschaft und Werkstofftechnik*, Vol. 51, No. 5, (2020), 550-557. <https://doi.org/10.1002/mawe.201900222>
  24. Meyghani, B. and Awang, M., "A novel tool path strategy for modelling complicated perpendicular curved movements", *Key Engineering Materials*, Vol. 796, (2019), 164-174. <https://doi.org/10.4028/www.scientific.net/KEM.796.164>
  25. Meyghani, B. and Awang, M., "Developing a finite element model for thermal analysis of friction stir welding (fsw) using hyperworks", in Advances in Material Sciences and Engineering, Singapore, Springer Singapore., (2020), 619-628. [https://doi.org/10.1007/978-981-13-8297-0\\_64](https://doi.org/10.1007/978-981-13-8297-0_64)
  26. Wang, K., "Transient temperature distribution in inertia welding of steels", *Welding Journal*, Vol. 49, (1970), 419s-426s.
  27. Qin, G., Geng, P., Zhou, J. and Zou, Z., "Modeling of thermo-mechanical coupling in linear friction welding of ni-based superalloy", *Materials & Design*, Vol. 172, (2019), 107766. <https://doi.org/10.1016/j.matdes.2019.107766>
  28. Okeke, S., Harrison, N. and Tong, M., "Thermomechanical modelling for the linear friction welding process of ni-based superalloy and verification", *Proceedings of the Institution of Mechanical Engineers, Part L: Journal of Materials: Design and Applications*, Vol. 234, No. 5, (2020), 796-815. <https://doi.org/10.1177/2F1464420719900780>
  29. Mohammed, M., Bennett, C., Shipway, P. and Hyde, T., "Optimization of heat transfer in the finite element process modelling of inertia friction welding of scmv and aermet 100", *WIT Transactions on Engineering Sciences*, Vol. 68, (2010), 253-265.
  30. Meyghani, B., Awang, M. and Wu, C., "Thermal analysis of friction stir welding with a complex curved welding seam", *International Journal of Engineering, Transactions A: Basics*, Vol. 32, No. 10, (2019), 1480-1484. Doi: <https://dx.doi.org/10.5829/ije.2019.32.10a.17>
  31. Meyghani, B. and Awang, M.B., "Prediction of the temperature distribution during friction stir welding (FSW) with a complex curved welding seam: Application in the automotive industry", MATEC Web Conference, Vol. 225, (2018), 01001. <https://doi.org/10.1051/mateconf/201822501001>

---

**Persian Abstract**

---

**چکیده**

شبیه سازی عددی جوشکاری اینرسی در دهه های گذشته مورد توجه تحقیقاتی زیادی قرار گرفته است. تغییر شکل مومسان بسیار بزرگ و رفتار اصطکاکی پیچیده این شبیه سازی را به چالش می کشد. در این مقاله مدل اصطکاک نورتون اصلاح شده است تا در یک مدل مکانیکی جامد محاسباتی جوشکاری اینرسی استفاده شود. برای جلوگیری از مشکل واپیچش مش از یک روش بازسازی مداوم استفاده می شود. نتایج نشان می دهد که بعد از 1.5 ثانیه دما به حداکثر مقدار  $1200^{\circ}\text{C}$  می رسد. پس از آن، الگوی کاهشی برای دمای جوش بروز می کند علاوه بر این، حداکثر تغییر شکل 6 میلی متر به دست می آید. مقادیر تنش به حداکثر 975 مگاپاسکال افزایش یافت. در نتیجه، پیش بینی موفقیت آمیز توزیع دما، تاریخچه حرارتی، تغییر شکل مومسان معادل، انقباض محوری و توزیع تنش ممکن می شود. مقایسه بین نتایج این مطالعه و اطلاعات گزارش شده در ادبیات نشان داد که اجرای روش پیشنهادی منجر به دست یابی به نتایج با دقت بالا می شود.

---